Reducing respiratory motion artifacts in fast 2D dynamic contrast enhanced MRI in liver using structural similarity

E.G.W. ter Voert[1], L. Heijmen[2], C.J.A. Punt[3], J.H.W. de Wilt[4], H.W.M. van Laarhoven[2,3], and A. Heerschap[1]

[1]Radiology, Radboud University Medical Centre, Nijmegen, Gelderland, Netherlands, [2]Medical Oncology, Radboud University Medical Centre, Nijmegen, Gelderland, Netherlands, [3]Medical Oncology, Academic Medical Center, University of Amsterdam, Amsterdam, Noord-Holland, Netherlands, [4]Surgery, Radboud University Medical Centre, Nijmegen, Gelderland, Netherlands

Target audience: Researchers involved in dynamic contrast enhanced MRI (DCE-MRI) of liver tumors.

Purpose: DCE-MRI with pharmacokinetic modeling provides information about tumor perfusion and vascular permeability and is often used to evaluate antivascular or antiangiogenesis therapies.[1,2] However, reproducibility of DCE-MRI in tumors in the liver is hampered by respiratory and cardiac motion. Common respiratory and cardiac gating cannot be applied because of the time variation in acquisition and the required sampling time of an arterial input function (AIF),which should be less than 2 seconds. 3D MRI of the whole liver and the aorta selected for an AIF, currently is too slow, as the AIF is a very important factor that should be measured accurately. With high-temporal-resolution 2D DCE-MRI, the AIF can be captured, but motion correction algorithms for the liver are prone to fail due to the gap between the slices or tumors that are (partially) moving in and out of a slice. The *aim of this study* was to implement and apply a structural similarity algorithm (SSIM) in the post-processing of DCE-MRI data to correct for movement artefacts.[3]

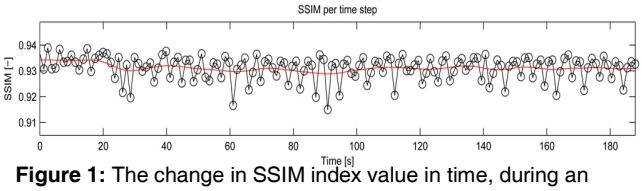

Figure 1: The change in SSIM index value in time, during an DCE-MRI measurement. These index values (circles) are plotted against the time that the dynamic DCE-MRI image was recorded.

Methods: Twenty patients with colorectal liver metastases were included and scheduled for two MRI examinations to assess reproducibility. During each visit Gd-DOTA was administered intravenously and its uptake in the tumor and the bolus passage in the aorta was monitored for 3 minutes (152 time points) using a T_1 weighted FLASH 2D MR sequence. The individual AIF was determined from the aorta by a modified version of the method described by Rijpkema et al.[4] To investigate the effect of motion on the reproducibility of K^{trans}, pharmacokinetic modeling (Tofts model) was performed twice for each DCE-MRI dataset. In one study all time points in the dataset were included, while in the other, time points with shifted tissue due to motion were excluded, as identified by the SSIM algorithm. The algorithm compares 2 input images and outputs a index value between -1 (dissimilar images) and 1 (equal images). The reproducibility of both studies were analyzed using the Bland & Altman method.

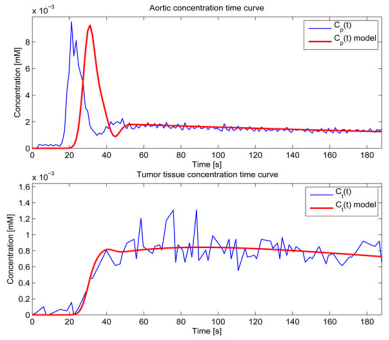

Figure 2: Top: A measured AIF (blue) and the fitted and time shifted AIF (red) from the aorta. Bottom: The measured tumor concentration vs. time curve (blue) and a fitted model (red).

Results: We calculated SSIM indices for each DCE-MRI image of a slice recorded at the different time points in the dynamic series (see Fig. 1 for an example). A high SSIM index value indicates that the compared images are almost similar, and thus approximately originate from the same location. Points below the red line are dissimilar and rejected. Note that there were about 13 cycles per minute, which corresponds to a normal human breathing cycle at rest. Figure 2 shows a typical AIF or $C_p(t)$ and a tumor concentration time curve, $C_t(t)$. Due to the rejection of data points, based on SSIM, the sampling frequency of the measured $C_t(t)$ curve is lower than that of the measured $C_p(t)$ curve. Figure 3 shows an example of calculated K^{trans} maps overlaid on an average T_1 weighted intensity image. As expected, the K^{trans} image with the SSIM applied (B) appears sharper and less blurred then the image without SSIM applied (A). Significant differences (Wilcoxon signed rank test, $p<0.025$) were observed between the median K^{trans} values in liver metastases corrected for motion with SSIM ($5.91 \times 10^{-3} \pm 3.22 \times 10^{-3}$ s^{-1}, median ± st.dev.) and without correction ($6.75 \times 10^{-3} \pm 3.34 \times 10^{-3}$ s^{-1}). The coefficient of repeatability for K^{trans} was 2.29×10^{-3} s^{-1} (38.7% of median) for liver metastases with and 3.58×10^{-3} s^{-1} (53.0% of median) without correction.

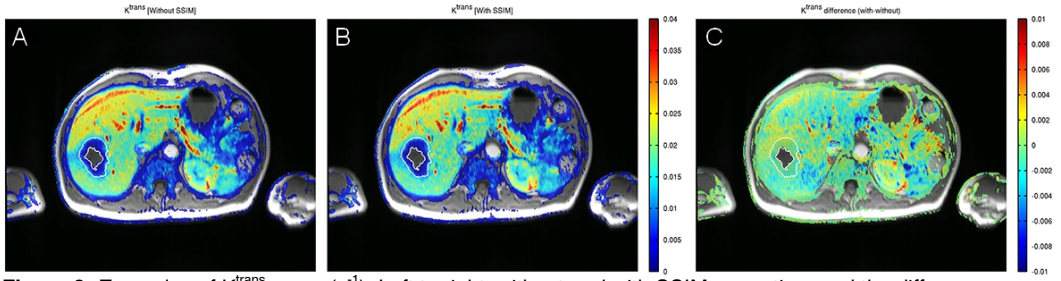

Figure 3: Examples of K^{trans} maps (s^{-1}). Left to right: without and with SSIM correction, and the difference, overlaid on average T_1 weighted intensity images. The tumor and its necrotic center are indicated by white lines.

Discussion:
Performing DCE-MRI on tumors in the liver is challenging due to respiratory motion. Liver tissue surrounding the tumor has a higher concentration of contrast agent compared to the tumor tissue. By reducing the contribution of surrounding liver tissue into the tumor ROI, the incorrectly measured higher concentrations in this ROI are also reduced. This explains the lower K^{trans} in the tumor ROI which we observed in the SIMM corrected dataset. It also resulted in a considerably improved coefficient of repeatability. The presented SSIM technique combined with the rejection of data points is fast and could easily be used in other abdominal areas or in combination with other MR acquisition protocols, e.g. MR spectroscopic imaging.

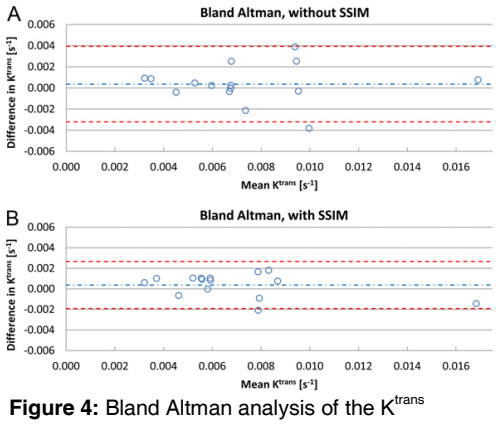

Figure 4: Bland Altman analysis of the K^{trans} values without (A) and with (B) SSIM correction. The blue dashed lines indicate the mean difference and the red dashed lines indicate the limits of agreement.

Conclusion: The structural similarity algorithm was successfully implemented into DCE-MRI post processing, allowing the rejection of motion corrupted time points. This substantially improved the reproducibility of the DCE-MRI parameter K^{trans} in the liver.

References:

1. Sourbron SP, Buckley DL., *Phys. Med. Biol.* 2012;57(2):R1. **2.** George ML, Dzik-Jurasz ASK, Padhani AR, et al., *Br. J. Surg.* 2001;88(12):1628–1636. **3.** Wang Z, Bovik AC, Sheikh HR, et al., *IEEE Trans. Image Process.* 2004;13(4):600 –612. **4.** Rijpkema M, Kaanders JHAM, Joosten FBM, et al., *J. Magn. Reson. Imaging.* 2001;14(4):457–463.